

# SEISMIC ASSESSMENT OF THE PRECODE HIGH RISE BUILDING FRAME USING THE PUSHOVER ANALYSIS

Karlo Grgurić<sup>(1)</sup>, Mario Uroš<sup>(2)</sup>

<sup>(1)</sup> Structural Engineer, XXL STEEL d.o.o., Zagreb, Croatia, [karlo.grguric12@gmail.com](mailto:karlo.grguric12@gmail.com)

<sup>(2)</sup> Associate professor, University of Zagreb, Faculty of Civil Engineering, Zagreb, Croatia, [mario.uros@grad.unizg.hr](mailto:mario.uros@grad.unizg.hr)

## Abstract

A large part of the housing stock of the Republic of Croatia consists of buildings that were built in the first half of the 20th century, when seismic regulations were poorly developed. Such buildings do not have quality details and have a high seismic risk. In this work a pushover analysis of a reinforced concrete historic high rise building in Zagreb was carried out in order to assess its seismic resistance. Given that the building is symmetrical in plan and has a frame structural system, one planar multi-story frame in weak direction was chosen for analyses. The quality of materials, dimensions of the cross-sections, and position of reinforcement in the elements were obtained from the building's archival documentation, along with non-destructive tests that were carried out on the building. A numerical model was established, and plastic hinges were defined for the columns and beams of the observed frame, with corresponding load-bearing capacity curves based on Eurocode 8-3. The analyses were carried out using the nonlinear static pushover analysis method (N2) in the ETABS software. The capacity curves of the structure and the significant structural damage index (SDI) were obtained for the observed direction of the building. At the end, a critical review of the analysis method and the original conception of the historical high rise building construction was made, and a proposal for strengthening the building was provided.

*Keywords:* seismic assessment, pushover analysis, high rise building

## 1. Introduction

Most of the buildings in the Lower Town of Zagreb were constructed at the end of the 19th and the beginning of the 20th century. Following a series of earthquakes in 2020 that struck the Zagreb (5,5 on the Richter scale [1]) and Petrinja (5,0 and 6,2 on the Richter scale [2]) areas, significant damage occurred to both non-structural and structural elements. The reason for this is that structural engineers of that period were not aware of designing structures to withstand seismic actions. This work will provide an assessment of the seismic resistance of a historic high-rise building in Zagreb dating back to the 1950s. The structural system of the mentioned high-rise building consists of a reinforced concrete frame in both dominant directions, with a lightly reinforced concrete stairwell core in the center [3]. The main deficiency of building is the insufficient amount of transverse reinforcement in the columns to resist lateral forces, with the dominant brittle shear failure. To obtain a reliable picture of the structure's behavior under seismic action, the nonlinear methods were used. In this work, the nonlinear pushover method will be applied. In addition to the nonlinear static method, a spectral analysis will also be performed. Given that the structure is symmetrical in plan, for simplicity of analysis, a one planar multi-story frame in the weaker direction of the structure will be extracted from the entire structure. The numerical analyses will be performed in software Etabs [4] on one planar multi-story frame using concentrated plastic approach with moment and shear plastic hinges in the columns and beams. The characteristics of materials, dimensions of the cross-sections, and position of reinforcement in the elements were obtained from the building's archival documentation [3], along with non-destructive tests that were carried out on the building.

The data on the quantity and distribution of reinforcement in the columns and beams is crucial for the application of the pushover method, as the reinforcement in the structural elements dictates the ductility of the elements and their seismic resistance. As an assessment of seismic resistance, the Significant Damage Index (SDI) will be obtained. The SDI index represents the ratio of the ground acceleration at which the structure reaches the limit state of Significant Damage (SD) and the ground acceleration according to regulations, considering a return period of 475 years [5].

## 2. Methodology of the analysis and structural modelling

### 2.1 Geometric and material properties of the structure

A one planar multi-story reinforced concrete frame (Ground floor + 10 floors) is analyzed, which is part of an existing reinforced concrete frame structure built in the 1950s in Zagreb [3]. The concrete material is C25/30 and reinforcement GA240, where the mean material values were applied ( $f_{cm} = f_{ck} + 8$  [N/mm<sup>2</sup>] and  $f_{ym} = 1,15 \cdot f_{yk}$ ). The modulus of elasticity of is 31 GPa for concrete, and 210 GPa for steel [3]. The geometry of the selected frame along with the corresponding reinforcement in the columns and beams is shown below [3]:

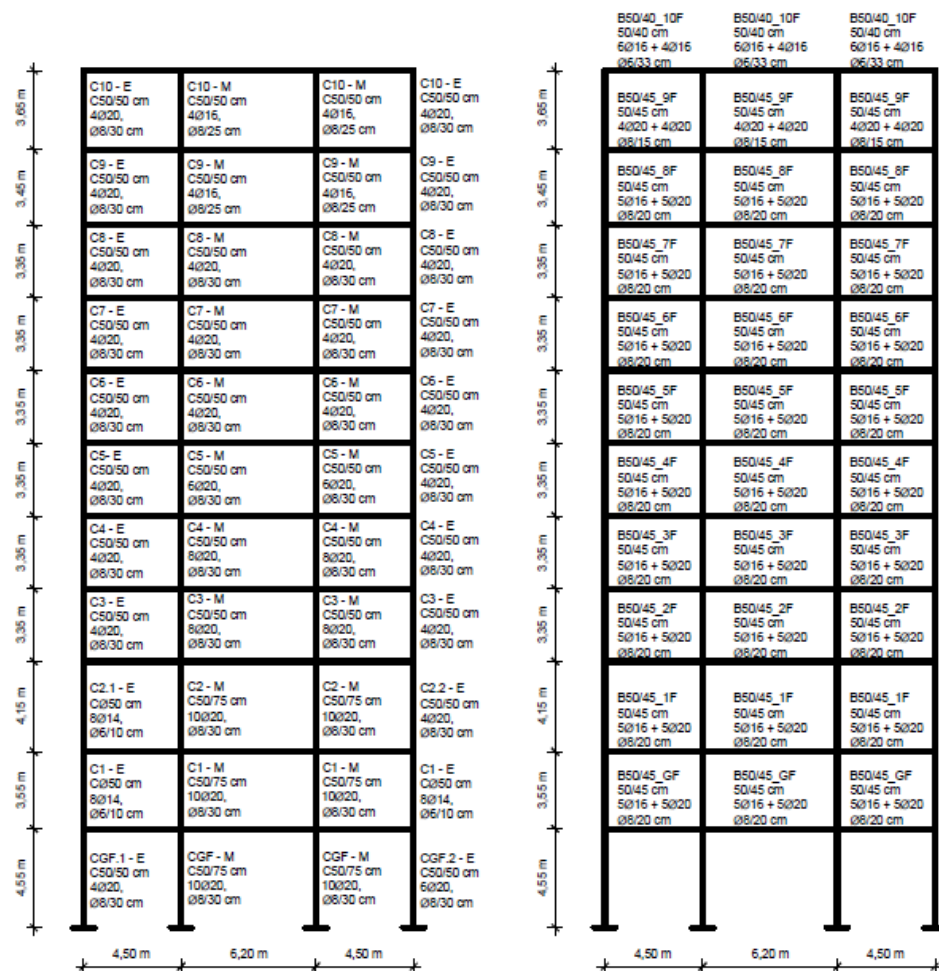


Figure 1. Geometric characteristics of elements and reinforcement of columns (left) and beams (right)

Regarding the labels of the elements, the first row indicates the position of the column or beam. The second row refers to the cross-sectional dimensions, the third row provides information about longitudinal reinforcement, and the fourth row specifies the transverse reinforcement of the columns and beams.

The first and third spans are length 4,5 m, while the middle span is 6,2 m. The floor heights vary and they are shown in Figure 1, with the total height of the structure being 39,45 m. The interaction with the ground has been simplified for the model using fixed hinge supports, as individual foundations are present. All load-bearing elements of the columns and beams are modeled as frame elements. The numerical model does not include the basement level, and it will not be considered in this study.

Below is the representation of the reinforcement in the characteristic column and beam [3]:

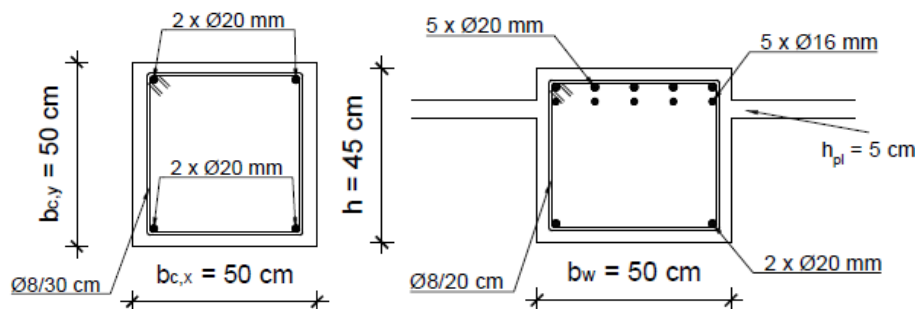


Figure 2. Reinforcement of the characteristic column (left) and beam (right)

## 2.2 Loads and actions

The loads acting on the structure include self-weight, additional permanent, live and seismic loads. To determine the exact load acting on the observed frame, it is necessary to convert loads such as additional permanent and live loads from surface ( $\text{kN/m}^2$ ) to linear ( $\text{kN/m}$ ), where the spacing of the main frames is 4,22 m [3]. The additional permanent load  $4,0 \text{ kN/m}^2$  [3] includes the weight of all layers and partition walls, resulting in a linear load of  $28,4 \text{ kN/m}$ . The live load varies depending on the floor level. The 1st and 2nd floors are office spaces, and according to [6], the live load is  $3,0 \text{ kN/m}^2$ , corresponding to a linear load of  $12,66 \text{ kN/m}$ , while the higher floors are residential, with a live load of  $2,0 \text{ kN/m}^2$ , corresponding to a linear load of  $8,44 \text{ kN/m}$ . As for the seismic load, the peak ground acceleration at the site of the building is  $0,254 \text{ g}$  [7] for a return period of 475 years, with a confidence factor of 1,0 [8] and a behavior factor of 1,5, which is used in the design response spectrum analysis. The low value of the behavior factor is taken because a low level of ductility in the cross-sections is assumed.

## 2.3 Modal analysis

The modal analysis was performed to determine the dynamic parameters of the structure (structural periods and modes of vibration). The total weight of the frame for the MASS combination, which accounts for self-weight, additional permanent, and 0,3 of the live load, is 7203 kN. Since this is a planar frame, the first mode of vibration is dominated by translation with a period of 2,97 s, where over 90% of the frame's mass is activated. Below is the deformation shape for the first two modes of vibration of the frame:

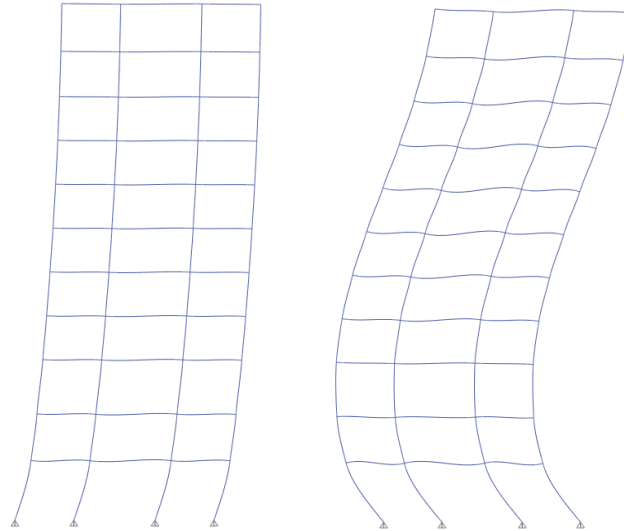


Figure 3. The first mode of vibration on the left ( $T_1 = 2,97$  s) and the second mode of vibration on the right ( $T_2 = 0,91$  s)

### 3. Methodology and structural modelling

#### 3.1 Geometric and material properties of the structure

For the analysis of the one planar multi-story structure, the [4] was used with certain assumptions and simplifications. The reduction of stiffness of elements according to [9] takes into account the occurrence of cracks in the elements. The shear and elastic bending stiffness of the beams, columns and RC plates were reduced to 50 %. [9]. Regarding the compressive strength of concrete cross-sections and the yield strength of reinforcement, their mean values were used.

#### 3.2 Properties of plastic hinges

Before assigning plastic hinges to the elements, it is necessary to properly define their parameters. To define the moment plastic hinges, it is first necessary to perform a cross-section analysis with the corresponding cross-sectional geometry, longitudinal and transverse reinforcement, as described in [10], in order to obtain the capacity curve of the cross-section from which the values of the section curvature at yielding and failure, as well as the plastic moment, are taken. According to [8], there are three limit states, which are Damage Limitation (DL), Significant Damage (SD) and Near Collapse (NR).

Furthermore, the curvatures at the limit states are determined according to [8]:

$$L_{pl} = 0,1 \cdot L_v + 0,17 \cdot h + 0,24 \cdot \frac{d_{bL} \cdot f_y (\text{MPa})}{\sqrt{f_c} (\text{MPa})} \quad (1)$$

$$\theta_y = \Phi_y \cdot \frac{L_v + a_{vz}}{3} + 0,0014 \cdot \left( 1 + 1,5 \cdot \frac{h}{L_v} \right) + \Phi_y \cdot \frac{d_{bL} \cdot f_y}{8 \cdot \sqrt{f_c}} \quad (2)$$

$$\theta_m = \frac{1}{\gamma_{el}} \cdot \left( \theta_y + (\Phi_u - \Phi_y) \cdot L_{pl} \cdot \left( 1 - \frac{0,5 \cdot L_{pl}}{L_V} \right) \right) \quad (3)$$

$$\theta_{SD} = \frac{3}{4} \cdot \theta_m \quad (4)$$

Where the coefficients are:

$L_{pl}$  – Length of the plastic zone

$L_V$  – (M/V) ratio at the end of the element

$h$  – Height

$d_{bL}$  – Diameter of tension reinforcement

$f_y$  – Yield strength of reinforcement

$f_c$  – Concrete compressive strength

$\theta_y$  – Curvature at the limit state of Damage Limitation

$\Phi_y$  – Curvature at yielding

$a_{vZ}$  – Displacement of the axial force diagram

$\theta_m$  – Curvature at the limit state of Near Collapse

$\gamma_{el} = 1,8$

$\Phi_u$  – Curvature at failure

$\theta_{SD}$  – Curvature at the limit state of Significant Damage

These values of the cross-sectional curvature at the limit states and the plastic moment are input data for defining plastic hinges in [4]. Moment plastic hinges are assigned to beams and columns at a distance of 0,5 m from the edges. To define shear plastic hinges, it is necessary to determine the design value of the cross-sectional resistance to shear force. This quantity is obtained according to [8]:

$$V_R = \frac{1}{\gamma_{el}} \left[ \frac{h-x}{2L_V} \cdot \min(N; 0,55 \cdot A_c \cdot f_c) + \left( 1 - 0,05 \cdot \min(5; \mu_{\Delta}^{pl}) \right) \right] \cdot \left[ 0,16 \cdot \max(0,5; 100 \cdot \varphi_{tot}) \cdot \left( 1 - 0,16 \cdot \left( 5; \frac{L_V}{h} \right) \right) \cdot \sqrt{f_c} \cdot A_c + V_W \right] [MN \text{ and } m] \quad (5)$$

Where the coefficients are:

$\gamma_{el} = 1,15$

$h$  – Height

$x$  – Compression zone depth

$N$  – Axial force

$A_c$  – Concrete cross-section area

$f_c$  – Concrete compressive strength

$\gamma_M = 1,5$

$L_V$  – (M/V) ratio at the end of the element

$\varphi_{tot}$  – Total longitudinal reinforcement ratio

$\mu_{\Delta}^{pl}$  – Ductility factor of transverse deflection due to shear stress or fiber rotation  $\theta$  normalized to fiber rotation at the moment of yielding  $\theta_y$ ;  $\mu_{\Delta}^{pl} = (\theta_u / \theta_y)$

$V_W$  – Contribution of transverse reinforcement to shear resistance

$$V_W = \varphi_w \cdot b_w \cdot z \cdot f_{yw} \quad (6)$$

Coefficients are:

$\varphi_w$  – Ratio of transverse reinforcement

$b_w$  – Width of the beam web

$z$  – Length of section internal lever arm

$f_{yw}$  – Yield strength of transverse reinforcement

Regarding the curvature at the previously mentioned limit states, since a brittle shear failure is assumed, a small value of curvature is assigned. This value must not be too small to avoid numerical issues during the nonlinear static analysis using plastic hinges. For the moment hinges of the columns, we have a symmetrical  $M_{pl}-\phi$  curve because the reinforcement in the columns is symmetrical. In the case of the beam, the situation is different due to the asymmetric reinforcement, so an asymmetric  $M_{pl}-\phi$  curve must be defined. The reason for this is that the moment from the MASS combination and the moment from the seismic combination may not act on the same side, so this approach covers both cases. The asymmetric  $M_{pl}-\phi$  curve is obtained by rotating the cross-section with the corresponding reinforcement by 180° during its definition, and the rest of the plastic hinge definition is the same as for the symmetrical  $M_{pl}-\phi$  curve. Below are graphical and tabular representations of the  $M_{pl}-\phi$  curves for the moment hinges of the columns and beams:

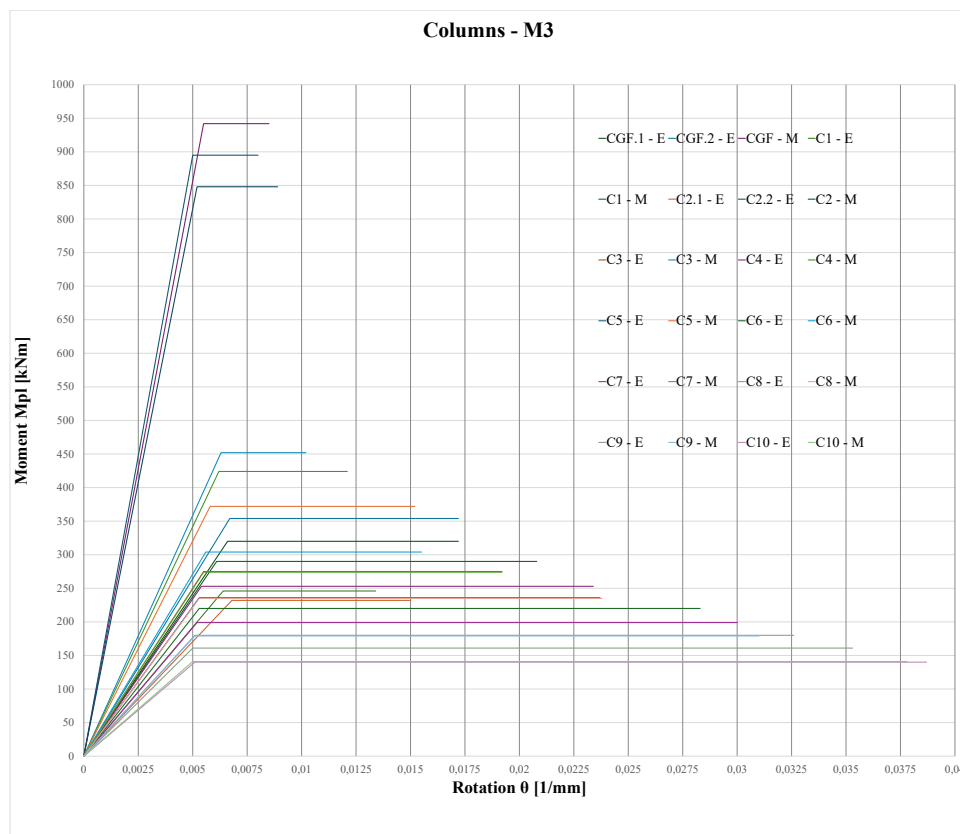


Figure 4.  $M_{pl} - \phi$  curves for columns

In Figure 4, it can be observed that the values of the middle columns of the ground floor and the first two floors deviate from the rest of the columns, showing a significantly higher value of the plastic moment and a lower capacity for cross-sectional rotation.

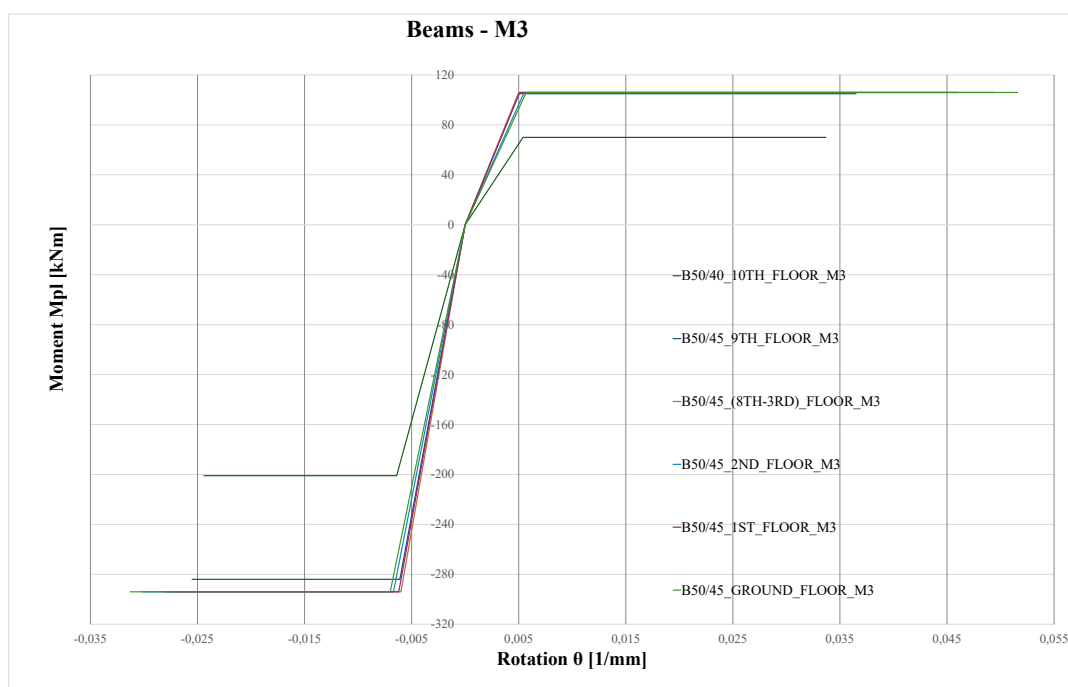


Figure 5.  $M_{pl} - \phi$  curves for beams

From Figure 5, it can be observed that the curves are identical for all beams with the same cross-sectional height, regardless of the floor they are located on. The only exception is the beam on the 10<sup>th</sup> floor, which has a cross-sectional height of 40 cm, and it stands out slightly.

Table 1 Tabular representation of column parameters

| MARK    | H (m) | L <sub>pl</sub> (m) | $\theta_y$<br>(1/mm) | $\theta_{SD}$<br>(1/mm) | $\theta_U$<br>(1/mm) | M <sub>pl</sub><br>(kNm) | P (kN) | V <sub>rd</sub> (kN) |
|---------|-------|---------------------|----------------------|-------------------------|----------------------|--------------------------|--------|----------------------|
| CGF.1-E | 4,55  | 0,54                | 0,0066               | 0,0129                  | 0,0172               | 320                      | 1153   | 45                   |
| CGF.2-E | 4,55  | 0,54                | 0,0067               | 0,0129                  | 0,0172               | 354                      | 1166   | 55                   |
| CGF-M   | 4,55  | 0,59                | 0,0055               | 0,0064                  | 0,0085               | 942                      | 2442   | 90                   |
| C1-E    | 3,55  | 0,42                | 0,0064               | 0,0101                  | 0,0134               | 246                      | 1053   | 55                   |
| C1-M    | 3,55  | 0,54                | 0,0050               | 0,0060                  | 0,0080               | 895                      | 2189   | 85                   |
| C2.1-E  | 4,15  | 0,45                | 0,0068               | 0,0112                  | 0,0150               | 232                      | 950    | 55                   |
| C2.2-E  | 4,15  | 0,52                | 0,0061               | 0,0156                  | 0,0208               | 290                      | 961    | 45                   |
| C2-M    | 4,15  | 0,57                | 0,0052               | 0,0067                  | 0,0089               | 848                      | 1948   | 85                   |
| C3-E    | 3,35  | 0,48                | 0,0055               | 0,0144                  | 0,0192               | 275                      | 853    | 45                   |
| C3-M    | 3,35  | 0,48                | 0,0063               | 0,0077                  | 0,0102               | 452                      | 1710   | 70                   |
| C4-E    | 3,35  | 0,48                | 0,0054               | 0,0176                  | 0,0234               | 253                      | 751    | 45                   |
| C4-M    | 3,35  | 0,48                | 0,0062               | 0,0091                  | 0,0121               | 424                      | 1492   | 70                   |
| C5-E    | 3,35  | 0,48                | 0,0053               | 0,0178                  | 0,0237               | 236                      | 646    | 45                   |
| C5-M    | 3,35  | 0,48                | 0,0058               | 0,0114                  | 0,0152               | 372                      | 1276   | 62                   |
| C6-E    | 3,35  | 0,48                | 0,0053               | 0,0212                  | 0,0283               | 220                      | 540    | 45                   |
| C6-M    | 3,35  | 0,48                | 0,0056               | 0,0116                  | 0,0155               | 304                      | 1062   | 50                   |
| C7-E    | 3,35  | 0,48                | 0,0052               | 0,0225                  | 0,0300               | 199                      | 432    | 45                   |
| C7-M    | 3,35  | 0,48                | 0,0055               | 0,0144                  | 0,0192               | 274                      | 849    | 50                   |
| C8-E    | 3,35  | 0,48                | 0,0051               | 0,0245                  | 0,0326               | 180                      | 324    | 45                   |
| C8-M    | 3,35  | 0,48                | 0,0053               | 0,0178                  | 0,0238               | 235                      | 638    | 50                   |
| C9-E    | 3,45  | 0,49                | 0,0050               | 0,0265                  | 0,0353               | 161                      | 214    | 45                   |
| C9-M    | 3,45  | 0,44                | 0,0051               | 0,0233                  | 0,0310               | 179                      | 427    | 50                   |
| C10-E   | 3,65  | 0,50                | 0,0051               | 0,0290                  | 0,0387               | 140                      | 103    | 45                   |
| C10-M   | 3,65  | 0,45                | 0,0050               | 0,0284                  | 0,0378               | 141                      | 217    | 50                   |

In Table 1, the parameters of the columns used in defining the plastic hinges are shown. It can be observed here that the governing failure mechanism will be due to shear force.

Table 2. Tabular representation of column parameters

| MARK                              | H (m) | L <sub>pl</sub> (m) | $\theta_y$ (1/mm) | $\theta_{SD}$ (1/mm) | $\theta_u$ (1/mm) | M <sub>pl</sub> (kNm) | V <sub>rd</sub> (kN) |
|-----------------------------------|-------|---------------------|-------------------|----------------------|-------------------|-----------------------|----------------------|
| B50/40_10 <sup>TH</sup> _FLOOR    | 3,65  | 0,43                | 0,0054            | 0,0252               | 0,0337            | 70                    | 150                  |
|                                   | 3,65  | 0,43                | -0,0064           | -0,0183              | -0,0244           | -201                  | 150                  |
| B50/45_9 <sup>TH</sup> _FLOOR     | 3,45  | 0,48                | 0,0050            | 0,0274               | 0,00365           | 105                   | 150                  |
|                                   | 3,45  | 0,48                | -0,0061           | -0,0192              | -0,0255           | -284                  | 150                  |
| B50/45_(8-3) <sup>TH</sup> _FLOOR | 3,35  | 0,47                | 0,0050            | 0,0336               | 0,0449            | 106                   | 150                  |
|                                   | 3,35  | 0,47                | -0,0060           | -0,0206              | -0,0275           | -294                  | 150                  |
| B50/45_2 <sup>ND</sup> _FLOOR     | 4,15  | 0,51                | 0,0055            | 0,0370               | 0,0494            | 106                   | 150                  |
|                                   | 4,15  | 0,51                | -0,0067           | -0,0226              | -0,0301           | -294                  | 150                  |
| B50/45_1 <sup>ST</sup> _FLOOR     | 3,55  | 0,48                | 0,0051            | 0,0345               | 0,0460            | 106                   | 150                  |
|                                   | 3,55  | 0,48                | -0,0062           | -0,0211              | -0,0282           | -294                  | 150                  |
| B50/45_GR_FLOOR                   | 4,55  | 0,53                | 0,0057            | 0,0387               | 0,0516            | 106                   | 150                  |
|                                   | 4,55  | 0,53                | -0,0070           | -0,0235              | -0,0313           | -294                  | 150                  |

In Table 2, the parameters of the mentioned asymmetric  $M_{pl}$ - $\phi$  curve can be observed. The shear capacity is also shown, and it is the same for all beams, regardless of the size of the cross-section or the position of the floor.

## 4. Results

A linear spectral analysis was performed, and the value of the maximum shear force 528 kN at the ground floor was obtained from the design spectrum for a return period of 475 years. The ratio of the maximum shear force to the structure's weight for the MASS combination is 7,33%.

The nonlinear pushover analysis was carried out with three loading cases. The first load case has the form caused by constant ground acceleration "Push\_Acceleration\_X," [5]. The second load case has a distribution corresponding to the quasi-static seismic force "Push\_Earthquake\_X," and the third load case is in the direction of the first modal shape and is named "Push\_Mode\_X" [5]. However, it is first necessary to balance the structure for vertical loads, which include its own weight, additional permanent load, and 0,3 of the live load, before proceeding with the pushover method [5]. Below is the capacity curve for reaching the limit state of significant damage, show for the numerical model with moment and shear plastic hinges, as these values are relevant for evaluating the seismic resistance of the structure. Along with the given structural parameters at the limit states, the deformation shape of the frame with the corresponding plastic hinges is shown. Plastic hinges for the Significant Damage State (SD) are marked in blue.

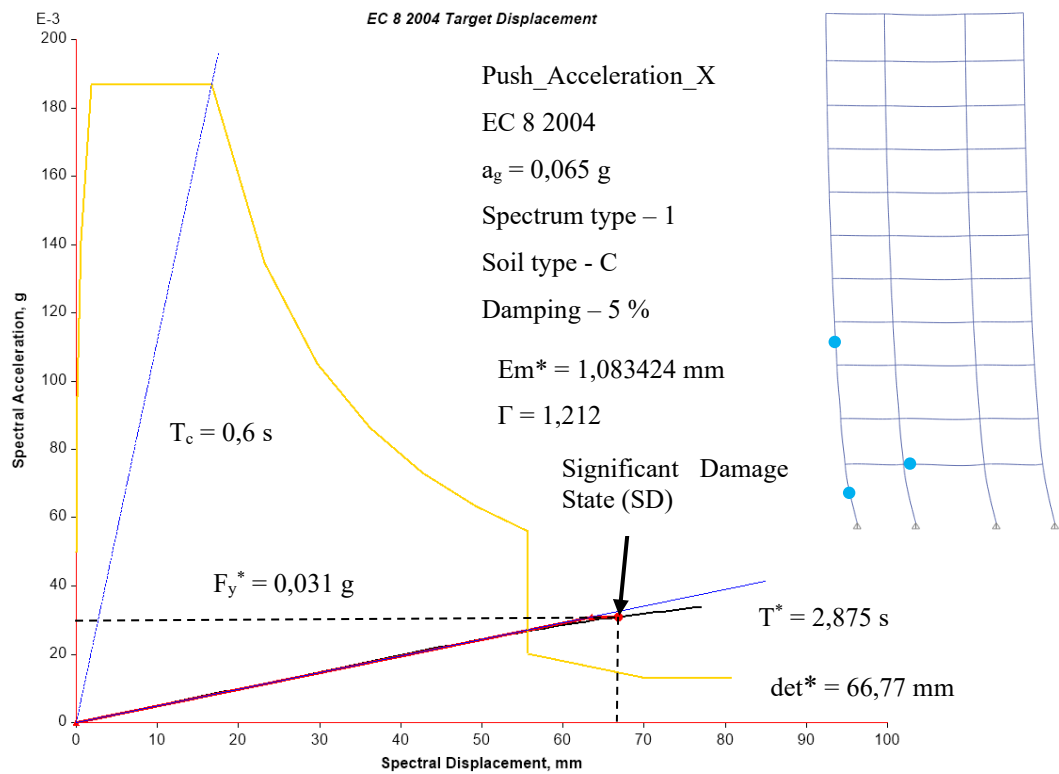


Figure 6 Capacity curve and deformation of the frame for the load case "Push\_Acceleration\_X"

For the load case "Push\_Acceleration\_X", the Significant Damage limit state is reached at a peak ground acceleration (PGA) of 0,065 g, and the Significant Damage Index (SDI) is 0,256. The force at this limit state is 204 kN, with a displacement of 80 mm.

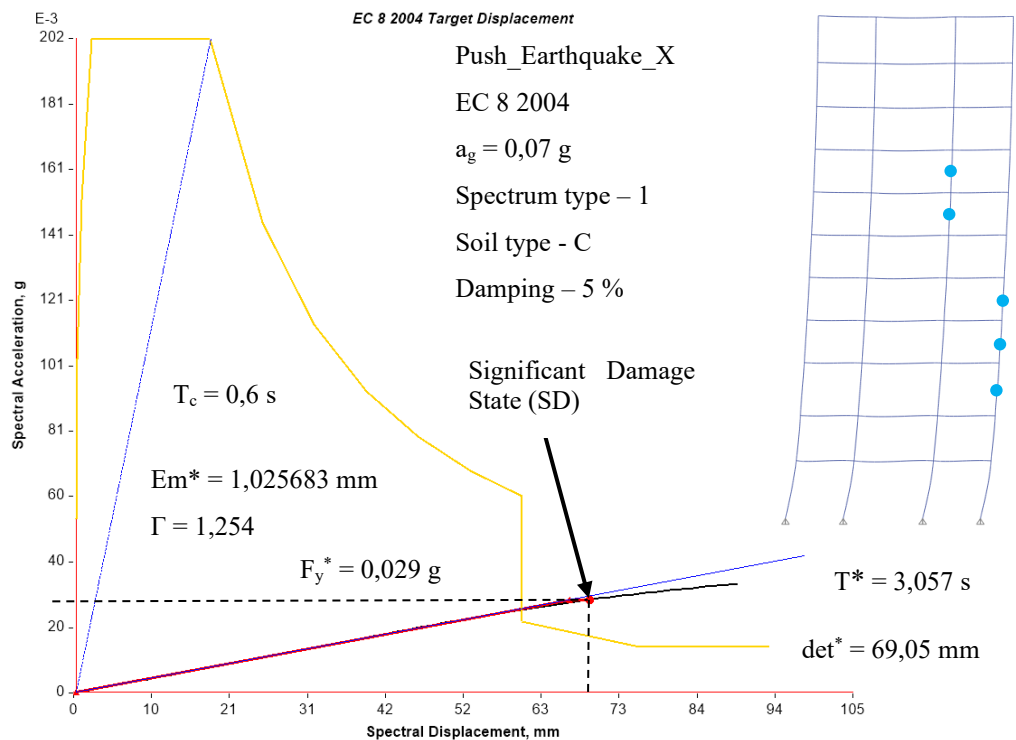


Figure 7 Capacity curve and deformation of the frame for the load case "Push\_Earthquake\_X"

For the load case "Push\_Earthquake\_X", the Significant Damage limit state occurs at a peak ground acceleration (PGA) of 0,07 g, and the Significant Damage Index (SDI) is 0,276. The force at this state is 185 kN, with a displacement of 86 mm.

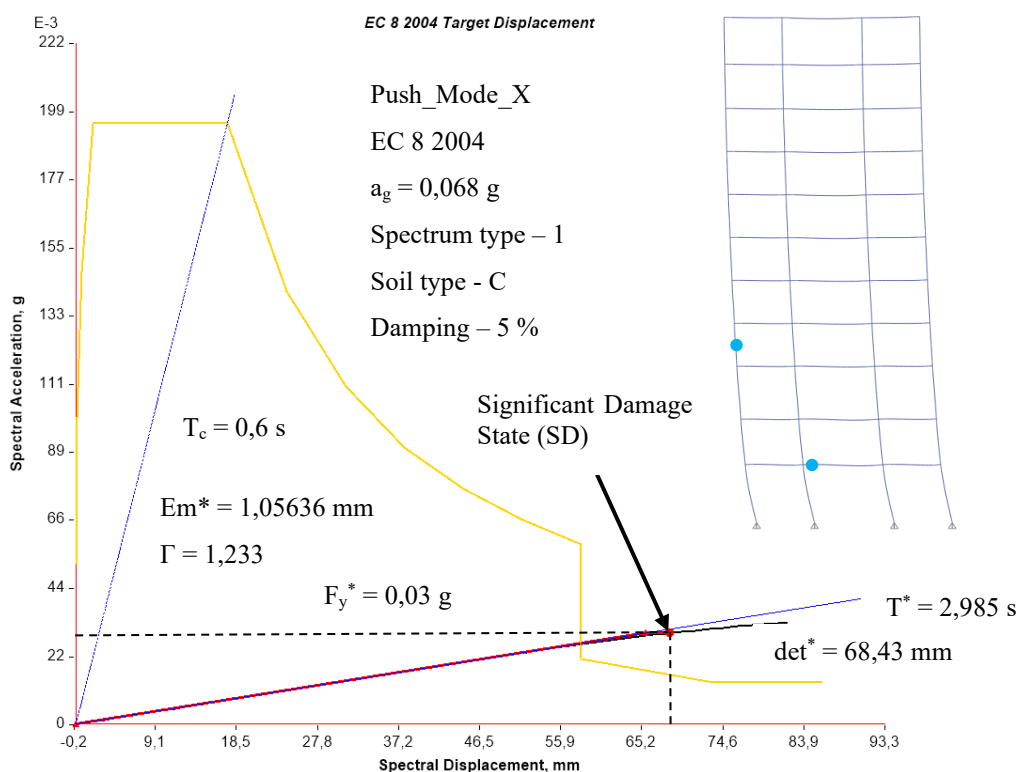


Figure 8 Capacity curve and deformation of the frame for the load case "Push\_Mode\_X"

For the load case "Push\_Mode\_X", the Significant Damage limit state of significant damage occurs at a peak ground acceleration (PGA) of 0,068 g, and the significant damage index (SDI) is 0,268. The force at this state is 194 kN, with a displacement of 84 mm.

## 5. Conclusions

The analysis of the one planar multi-story frame, based on the displacements of the frame, has shown that the observed frame lacks sufficient ductility. The limiting factor is that the building does not have adequate transverse reinforcement and reinforcement detailing to withstand seismic forces without significant damage to elements. The structural system of the mentioned high-rise building consists of a reinforced concrete frame in both dominant directions, with a lightly reinforced concrete stairwell core in the center. The observed reinforced concrete one planar multi-story frame has a relatively high first vibration period of 2,97 s, with dominant translation and mass activation over 90%. The load-bearing capacity of the building is exhausted by shear failure of the concrete due to transverse forces, and this mechanism is brittle and very dangerous as it leads to sudden and unexpected failure of structural elements. The nonlinear static method showed a peak ground acceleration of 0,065 g at which a Significant Damage (SD) limit state occurs. The result is far from satisfactory considering today's seismic regulations. The SDI factor obtained at the Significant Damage (SD) limit state is 0,256. If shear brittle failure is prevented in the structure and a bending failure mechanism is allowed at the joints, the seismic resistance of the structure is significantly increased, as a much more ductile failure mechanism of the elements is achieved. To achieve this, it is necessary to wrap the frame joints with FRP strips or fabrics. This method increases the ductility and shear resistance of the structure, thereby reducing the risk of brittle failure and improving the seismic resistance of the building.

## Acknowledgements

This work was created as part of the Master's thesis titled "ASSESSMENT OF THE LOAD BEARING CAPACITY OF THE EXISTING HIGH RISE BUILDING USING THE PUSHOVER ANALYSIS" in collaboration with my mentor, Associate Professor Mario Uroš.

## References

- [1] Two years since the Zagreb earthquake. University of Zagreb, Faculty of Science – Department of Geophysics. Available online: [https://www.pmf.unizg.hr/geof/seizmoloska\\_sluzba/o\\_zagrebackom\\_potresu\\_2020](https://www.pmf.unizg.hr/geof/seizmoloska_sluzba/o_zagrebackom_potresu_2020) (accessed on 12th February 2025)
- [2] Analysis of accelerograms for the earthquakes near Petrinja. University of Zagreb, Faculty of Science – Department of Geophysics. Available online: [https://www.pmf.unizg.hr/geof/seizmoloska\\_sluzba/potresi\\_kod\\_petrinje\\_2020#](https://www.pmf.unizg.hr/geof/seizmoloska_sluzba/potresi_kod_petrinje_2020#) (accessed on 12th February 2025)
- [3] Croatian Museum of Architecture, Croatian Academy of Sciences and Arts: OAF Drago Ibler, (accessed on 25th September 2023)
- [4] ETABS, version 20, Computers and Structures, Inc., Berkeley, California, USA, 2022.
- [5] Uroš M., Todorčić M., Crnogorac M., Atalić J., Šavor Novak M., Lakušić S. (eds.), Earthquake Engineering: Restoration of Masonry Buildings, Zagreb: University of Zagreb, Faculty of Civil Engineering, 2021.
- [6] EN1991, Eurocode 1: Actions on Structures—Part 1-1: General Actions—Densities, Self-weight, Imposed Loads for Buildings; European Committee for Standardization (CEN): Brussels, 2002.
- [7] Seismic zoning maps of the Republic of Croatia, (accessed on 12th February 2025)
- [8] EN1998—Part 3, Eurocode 8: Design of Structures for Earthquake Resistance—Part 3: Assessment and retrofitting of buildings; European Committee for Standardization (CEN): Brussels, Belgium, 2005.
- [9] EN1998—Part 1, Eurocode 8: Design of Structures for Earthquake Resistance—Part 1: General Rules, Seismic Actions and Rules for Buildings; European Committee for Standardization (CEN): Brussels, Belgium, 2004.
- [10] SAP2000, version 18, Computers and Structures, Inc., Berkeley, California, USA, 2016.